Electronic and Magnetic Properties of Neutral and Charged Quinone and Plastoquinone Radicals

Leif A. Eriksson,*,† Fahmi Himo,† Per E. M. Siegbahn,† and Gerald T. Babcock‡

Department of Physics, Stockholm University, Box 6730, S-113 85 Stockholm, Sweden, and Department of Chemistry, Michigan State University, East Lansing, Michigan 48824-1322

Received: June 23, 1997; In Final Form: September 24, 1997[⊗]

Semiquinones are of vital importance in a number of biological systems, where they act as mediators in electron transport. In the present work we have employed hybrid and gradient-corrected density functional methods to investigate theoretically the electronic and magnetic properties of 1,4-benzoquinone, its ethylated counterpart, and a model plastoquinone. The structures are optimized at the B3LYP/6-311G(d,p) level, followed by single-point B3LYP/6-311+G(2df,p) and PWP86/6-311G(2d,p) energy and hyperfine properties calculations. Hydrogen bonding to the quinone and plastoquinone oxygens are modeled. Based on comparisons with experimental ESR data, the results strongly support the presence of hydrogen-bonding moieties to both oxygens of the quinone radical anion Q_A^- in photosystem II. These hydrogen-bonding groups are shown to increase the electron affinity of the quinones by ca. 0.6 eV and are hence of crucial importance for the functionality of the entire photochemical process. As a final part of the paper, we outline briefly the energetics involved in the electron−proton/H-atom transport in the quinone pool of the thylakoid membranes, linking photosystem II to photosystem I.

Introduction

Quinones are known to play a major role in electron-transfer reactions of photosynthesis and respiration and have been detected in a large number of enzymes and proteins. The key property of quinones is the capacity to act as electron acceptors, caused by a substantial electron affinity. At the same time, the proton affinity of the radical anion Q^- is high, which, in combination with an unusually low bond dissociation energy of the hydroxy hydrogen in QH, allows it to function as a $H^+ + e^- \rightarrow$ H atom transporter.

In photosystem II (PSII), two plastoquinones Q_A and Q_B act as electron mediators between the light-oxidized chlorophyll reaction center P_{680} and the plastoquinone pool (Q/QH_2) of the thylakoid membranes.[1] The electrons delivered from water by P_{680} are used by the Q/QH_2 pool to carry protons across the membrane to the cytochrome b_6f complex. The photosynthetic bacterial reaction center has analogies to PSII in the quinone acceptor region, and for the bacterial system, we have detailed crystallographic information.[2−4] For PSII, however, a crystal structure is lacking, and little is known about, for example, the exact structural arrangements, bond distances in the various functional groups, and presence or absence of hydrogen bonding. Although some insight into these issues is beginning to emerge (see below), model systems and theoretical modeling of the constituent fragments of the protein system can play a crucial role in increasing our understanding of the function and control of quinones in photosynthetic processes and by extension, the other systems in which these ubiquitous cofactors occur.

A great number of experimental studies of model semiquinones have appeared in the literature.[5−13] Detailed results have been reported for the ^1H, ^{13}C, and ^{17}O hyperfine coupling constants (hfcc), the effects of different solvents on the hyperfine properties of the systems, the effects of different substituents, and the occurence of hydrogen bonding to the quinone anion radical in these model systems. Magnetic resonance techniques have also served as invaluable tools to reveal detailed information of the structures and functions of a number of enzymes and proteins directly. Recently, Rigby et al.[14] and Lubitz and co-workers[15] managed to obtain EPR and ENDOR measurements of the hyperfine properties of the plastoquinone anion radical Q_A^- in PSII and of plastoquinone-9 anion model systems (PQ-9) in frozen 2-propanol. In addition, Zheng and Dismukes presented a comparison of the local rotational arrangement of the semiquinones in purple bacteria and in PSII of higher plants from an EPR study of the β-proton hyperfine structures.[16]

Much of the previous theoretical work on quinones has focused on comparisons of geometries and vibrational spectra of neutral and anionic 1,4-benzoquinone,[17−20] the electron-transfer processes and redox potentials of model plastoquinones,[21−23] the hyperfine splittings of quinone radical anions,[19,24,25] or the effects on the hyperfine structures of different dielectric media.[26] Some of the most recent studies are those by Wheeler and co-workers[18−20] and by O'Malley and Collins[25] on geometries, vibrational frequencies, and isotropic hyperfine data of the anion radicals of 1,4-benzoquinone, including effects of methylation and hydrogen bonding, and different plastosemiquinone models.

We have recently initiated a series of detailed theoretical studies of the functions of fundamental biophysical systems such as the metallocenters in PSII, methyl monoxygenase (MMO), and ribonucleotide reductase (RNR), and the reactions and properties of amino acid radicals in PSII, RNR, cytochrome *c* peroxidase (CcP), and DNA photolyase.[27−30] In this work, gradient-corrected density functional theory (DFT) or hybrid Hartree−Fock/DFT methods, such as PWP86 and B3LYP, respectively, have been found to be highly suitable also for studies of biophysical systems. We have here chosen to study the structures, energetics, and properties of a large number of 1,4-benzoquinone model systems by means of gradient-corrected and hybrid DFT methods by using basis sets of very high quality (valence triple-zeta plus polarization) throughout.

The systems investigated are the neutral 1,4-benzoquinone ground-state singlet and first excited state triplet (Q, $Q^\dagger$), the radical anion ($Q^{\bullet -}$), the radical cation ($Q^{\bullet +}$), and the singly and

† Stockholm University.
‡ Michigan State University.
[⊗] Abstract published in *Advance ACS Abstracts,* November 15, 1997.

S1089-5639(97)02045-8 CCC: $14.00

doubly protonated anion radical ($QH^{\bullet}$ and $QH_2^{\bullet+}$). Hydrogen-bonding water molecules are included in the studies of Q^-, and the effects of the hydrocarbon tail at the 3-position are investigated for the systems denoted QEt^-, QEt^+, and QEtH. We also investigate a Q_A^- plastoquinone anion model (5-ethyl-2,3-methyl-1,4-benzoquinone; psQ^-) and the effects of hydrogen bonding on its hyperfine properties. Finally, we describe the energetics involved in the different stages of the electron−proton transporting function of the quinone in thylakoid membranes.

Methods

All geometry optimizations, including those of the hydrogen-bonded systems, and subsequent vibrational frequency calculations, were performed at the B3LYP/6-311G(d,p) level. These were followed by single-point calculations of energies, spin distributions, and hyperfine properties at the B3LYP/6-311+G-(2df,p) and PWP86/6-311G(2d,p) levels. The B3LYP hybrid density functional consists of a linear combination of Hartree−Fock exchange with local and gradient-corrected DFT exhange (S,[31] B88[32]) and local and gradient-corrected DFT correlation (VWN,[33] LYP[34]). The exact relation between the different contributions was determined by Becke (although originally using a different gradient correction to the correlation than the LYP functional), from a least-squares fit to atomization energies, ionization potentials, and electron affinities for the G1 set of molecules.[35] The PWP86 functional, on the other hand, is a pure DFT functional, with gradient corrections to the S-VWN local density functional as developed by Perdew and Wang for the exchange part[36] and by Perdew to the correlation.[37] The B3LYP calculations were performed by using the Gaussian 94 program,[38] whereas for the PWP86 calculations we used the deMon code.[39]

The combination of the PWP86 DFT functional with the 6-311G(2d,p) basis set for the evaluation of radical hyperfine properties was recently introduced,[40] and found to be highly appropriate. The accuracy in predicted α-proton hyperfine coupling constants for a number of substituted phenoxyl and benzyl radicals was within 95% of experiment, with a slightly larger deviation for non-hydrogen substituents and β-protons.[40] From the single-point PWP86/6-311G(2d,p) hyperfine calculations, we obtain both the isotropic and anisotropic hyperfine parts.

The hyperfine coupling constants (hfcc's) result from magnetic interaction between the unpaired electron(s) of the radical and the magnetic nuclei of the sample (here: ^{1}H, ^{13}C, and ^{17}O). The magnetic hyperfine tensor can be separated into two parts: an isotropic (Fermi contact) component and a remaining anisotropic part. The isotropic hfcc's result from a direct contact interaction and can be computed using the unpaired electron density at the position of the nuclei:

$$A_{\mathrm{iso}}(N) = \frac{4\pi}{3} g_e \beta_e g_N \beta_N \langle S_z \rangle^{-1} \rho^{\alpha-\beta}(0)$$

where g_e and β_e are the electronic g-factor (usually taken as the free electron value, 2.0023) and the Bohr magneton, respectively, g_N and β_N are the corresponding nuclear terms, S_z represents the total electron spin of the system (=1/2 for doublet radicals), and $\rho^{\alpha-\beta}(0)$ is the unpaired spin density at the nucleus ($r = 0$). For the anisotropic (dipolar) part, an ijth component can be obtained as

$$T_{ij}(N) = \frac{1}{2} g_e \beta_e g_N \beta_N \langle S_z \rangle^{-1} \sum_{\mu,\nu} P_{\mu,\nu}^{\alpha-\beta} \langle \phi_\mu | r_{kN}^{-5} (r_{kN}^2 \delta_{i,j} - 3 r_{kN,i} r_{kN,j}) | \phi_\nu \rangle$$

TABLE 1: B3LYP/6-311G(d,p) Optimized Geometries (Å and deg) for the 1,4-Benzoquinones Investigated in the Present Study. Energies from Single-Point B3LYP/6-311+G(2df,p) Calculations

system: multipl.:	Q[a] 1	Q† 3	Q^- 2	QH 2	*c*-QH_2^+ 2	*t*-QH_2^+ 2	Q^+ 2
C1−C2	1.486	1.456	1.452	1.411	1.426	1.424	1.512
C2−C3	1.339	1.352	1.369	1.372	1.367	1.365	1.321
C3−C4	1.486	1.456	1.452	1.453	1.426	1.428	1.512
C4−C5	1.486	1.456	1.452	1.454	1.427	1.424	1.512
C5−C6	1.339	1.352	1.369	1.369	1.362	1.365	1.321
C6−C1	1.486	1.456	1.452	1.413	1.427	1.428	1.512
C1−O1	1.218	1.250	1.262	1.352	1.317	1.316	1.198
C4−O4	1.218	1.250	1.262	1.249	1.317	1.316	1.198
O1−H1				0.962	0.970	0.970	
O4−H4					0.970	0.970	
C6−C1−C2	117.1	115.6	114.4	120.6	120.7	120.7	116.9
C1−C2−C3	121.5	122.2	122.8	120.5	119.6	119.5	121.6
C2−C3−C4	121.5	122.2	122.8	121.5	119.6	119.7	121.6
C3−C4−C5	117.1	115.6	114.4	116.2	120.7	120.7	116.9
C4−C5−C6	121.5	122.2	122.8	121.7	119.7	119.5	121.6
C5−C6−C1	121.5	122.2	122.8	119.9	119.7	119.7	121.6
H1−O1−C1				109.9	113.2	113.2	
H4−O4−C4					113.2	113.2	
H1−O1−C1−C2				0.0	0.0	0.0	
H4−O4−C4−C3					0.0	180.0	
ΔE (kcal)	0.0[b]	+47.1	−49.2	−379.3	−601.7	−601.9	+227.7

[a] Exp. geometry: C1−O1 = 1.225, C1−C2 = 1.481, C2−C3 = 1.344, C6−C1−C2 = 118.1.[41] [b] Absolute energy for neutral Q: −381.582963 au. All energies relative that of Q.

The integral expression is the quantum analogue of the classical expression for interacting dipoles and gives an estimate of the asymmetry of the spin distribution around each nucleus. Comparing computed and measured hfcc's for a number of conformers, theory can be used to identify the nature and geometry of the experimental system under study. The hyperfine structure also reveals valuable information on the presence or absence of hydrogen bonding and the distribution of unpaired spin in the system. Having found an appropriate theoretical model that reproduces the experimental observations, this can then be used to extract further information regarding, for example, reaction energies, interaction with neighboring molecules/groups, and intramolecular charge distributions.

Results and Discussion

A. 1,4-Benzoquinones. *Geometries, Energies, and Vibrational Frequencies.* In Tables 1 and 2 we present the B3LYP/6-311G(d,p) optimized geometries of the quinones (Table 1) and ethylquinones and plastoquinone (Table 2), respectively. In Table 3 we summarize some of the fundamental energetics of 1,4-benzoquinone and related systems. Figure 1 displays the various quinone radicals, including the spin density distributions from the PWP86/6-311G(2d,p)//B3LYP/6-311G(d,p) calculations (A−J) and the numbering scheme employed (K).

1,4-Benzoquinone (Q) displays two distinctive types of carbon−carbon bonds. Those connecting to C1 and C4 (cf. Figure 1) have more single bond character ($R \simeq 1.49$ Å), and the two intermediate bonds C2−C3 and C5−C6 display more double-bond character ($R \simeq 1.34$ Å). The C−O distances are typical for carbon−oxygen double bonds of aldehydes and ketones, 1.22 Å. The C−C(O)−C bond angles are slightly less than 120°. The optimized parameters for Q agree well with experimental data.[41] Upon excitation to the lowest exited triplet state, the C═O and C═C "double bonds" become elongated and the C−C single bonds slightly shorter; all changes are within ±0.04 Å. The excitation energy is just above 2 eV.

The same types of geometric changes occur upon addition of an electron to 1,4-benzoquinone. The electron affinity of Q is rather high, 2.13 eV; after ZPE corrections, the electron

TABLE 2: B3LYP/6-311G(d,p) Optimized Geometries (Å and deg) for the Three 5-Ethyl-1,4-benzoquinones and the Plastoquinine Anion Model Investigated in the Present Work

	QEt^-	QEtH	QEt^+	psQ^-
C1−C2	1.449	1.409	1.503	1.460
C2−C3	1.370	1.371	1.326	1.379
C3−C4	1.446	1.450	1.501	1.459
C4−C5	1.464	1.470	1.533	1.458
C5−C6	1.373	1.374	1.338	1.369
C6−C1	1.453	1.411	1.504	1.447
C5−C7	1.512	1.505	1.500	1.513
C7−C8	1.529	1.528	1.523	1.530
C9−C2				1.508
C10−C3				1.509
C1−O1	1.262	1.354	1.202	1.264
C4−O4	1.264	1.249	1.198	1.266
O1−H1		0.964		
C6−C1−C2	114.9	121.0	117.4	116.1
C1−C2−C3	122.1	119.4	121.0	121.2
C2−C3−C4	122.9	121.7	121.9	121.9
C3−C4−C5	115.7	117.3	116.8	116.9
C4−C5−C6	120.6	119.4	119.2	120.4
C5−C6−C1	123.8	121.1	122.1	123.5
C7−C5−C4	115.4	116.7	114.0	115.7
C8−C7−C5	116.5	116.4	116.3	116.3
H1−O1−C1		109.8		
H1−O1−C1−C2		0.0		

affinity is adjusted to 2.04 eV (exp: 1.91 eV[42]). This can be compared with, for example, 1.01 eV for nitrobenzene, 1.10 eV for phenyl, 1.70 eV for anilide, and 2.25 eV for phenoxyl.[41] This implies a good ability of the system to act as an electron sink (electron acceptor) in electron-transfer reactions. The obtained geometry of Q^- agrees closely with those reported in previous B3LYP and ROHF calculations.[18,25] For the quinone cation radical, the geometric changes are opposite those of Q^+ and Q^-; that is, the bonds with double-bond character shorten, whereas the C−C single bonds increase to 1.512 Å. The ionization potential is nearly 10 eV, which is higher than essentially all other substituted benzenes known.[41,43]

Adding a hydrogen to Q (or a proton to Q^-) causes a distortion of the symmetric structure. The fragment close to the protonated oxygen displays the largest modifications to the geometry, caused by the new single bond formed between C1 and O1. The C6−C1−C2 bond angle increases to ca. 120°. The geometry of the unsubstituted fragment is highly similar to that of Q^-. Adding a proton to the second oxygen to form QH_2^+ causes the same type of local distortions around C4, whereas the C2═C3 and C5═C6 double bonds remain similar to those computed for Q^-. There are very minor geometric differences between the cis and trans forms of QH_2^+; energetically the trans form is more stable by ca 0.2 kcal/mol. The computed proton affinities (PA) of Q^- and QH (forming QH and QH_2^+, respectively) are 16.44 and 9.65 eV; again this is unusually high for the first PA, whereas "normal" for the second. Possibly this high PA is related to the fact that calculations are performed in vacuum, neglecting possible solvent interactions. The O−H bond dissociation energy in QH is 64.2 kcal/mol, which is rather low. For water, the O−H bond dissociation energy is 119.1 kcal/mol, in formic acid it is 105.9 kcal/mol, in methanol 104.3 kcal/mol, and in phenol 86.5 kcal/mol.[41]

The vibrational frequencies (not listed) showed that all 1,4-benzoquinones, including the neutral system, have a large number of low-frequency modes. These correspond mainly to ring bending and rocking motions. The intermediate band at 1500−1800 cm^{-1} includes the C═O stretching vibrations, and the high-frequency modes (>3000 cm^{-1}) arise from the C−H stretches. All frequencies of the optimized structures are real, indicating true minima on the potential surfaces, and agree with previous theoretical calculations. For detailed analyses and assignements of each mode we refer to, for example, refs 17−19.

TABLE 3: Summary of Energetics of the 1,4-Benzoquinone System. Calculations at B3LYP/6-311+G(2df,p)// 6-311G(d,p) Level

system	energy[a]	ΔZPE	exp (eV)
Q	ionization potential: 9.88 eV	2.27 kcal	10.04 ± 0.18[b]
	electron affinity: 2.13 eV	1.14 kcal	1.91[c]
	excitation energy: 2.04 eV		
Q^-	(electron affinity: −3.28 eV)		
	proton affinity: 16.44 eV	8.11 kcal	
	strength, 1st H-bond: 12.63 kcal/mol[d]	2.45 kcal	
	strength, 2nd H-bond: 11.74 kcal/mol[e]		
QH	electron affinity: 1.84 eV		
	proton affinity: 9.65 eV	8.62 kcal	
	O-H bond strength: 64.2 kcal/mol	6.97 kcal	
QH^-	proton affinity: 15.48 eV		
	O-H bond strength: 57.6 kcal/mol		
QH_2	ionization potential: 7.67 eV		
	O-H bond strength: 84.5 kcal/mol		
psQ	electron affinity: 1.85 eV		
$Q(H_2O)_2$	electron affinity: 2.76 eV		
$psQ(H_2O)_2$	electron affinity: 2.32 eV[f]		

[a] Without ZPE corrections. [b] Reference 43. [c] Reference 42. [d] Obtained as difference between full complex and $Q^{\bullet-}H_2O + H_2O$ at infinite separation. [e] Obtained as difference between full complex and $Q^- + H_2O$ at infinite separation. [f] Obtained at B3LYP/6-311G(d,p) level. At this level, the EA of psQ is 1.65 eV, compared with 1.85 eV using the larger basis set.

Ethylation (Table 2) cause the quinone molecules to distort geometrically. The largest distortions occur in the C4−C5 bonds (ethyl group bonded to C5), which become elongated by ca. 0.02 Å compared with the nonalkylated systems. In the cation radical, QEt^+, the changes to the CC double bonds are the largest, and the two C═O bonds become unequal as a result of the alkylation.

Hydrogen bonding causes local distortions at the CC(O)C fragment involved in the bonding. Compared with the free 1,4-benzoquinone anion radical, the H-bond causes an increase in the C−C−C bond angle by ca. 1°, the C−C bonds shorten from 1.452 to ca. 1.446 Å, and the C═O bond increases by ca. 0.01 Å. In both the singly and the doubly hydrogen-bonded cases the water molecule H−O fragments lie in the quinone ring plane, whereas the hydrogen not involved in the H-bond points almost perpendicular to the ring plane. The O1−H−O angle is 168°, and the C1−O1−H angle 116°. The O1−H hydrogen bond distance is 1.760 Å (single water) and 1.777 Å (two waters). Again, the geometries of the H-bonding complexes are highly similar to the B3LYP/6-31+G(d) geometries obtained by O'Malley and Collins on $Q^-(MeOH)_2$.[25] The H-bonding distance is slightly longer in the present calculations, and the C1−O1−H angle is ca. 10° smaller. The dissociation energy of the first hydrogen bond to Q^- is 12.6 kcal/mol, and the second 11.7 kcal/mol. The ZPE correction reduces the first hydrogen bond by ca. 2.45 kcal/mol; a roughly equal amount can be assumed also for the second one. Basis set superposition errors (BSSEs) were not calculated.

The presence of the two hydrogen-bonding moieties are furthermore of vital importance for the energetics. As can be seen from Table 3, the two water molecules increase the electron affinity of Q by more than 0.6 eV (ca. 14 kcal/mol), from 2.13 to 2.76 eV.

Spin and Charge Distributions. The spin density distributions obtained from Mulliken population analyses are presented in Figure 1. The spin populations are less than 0.01 (absolute

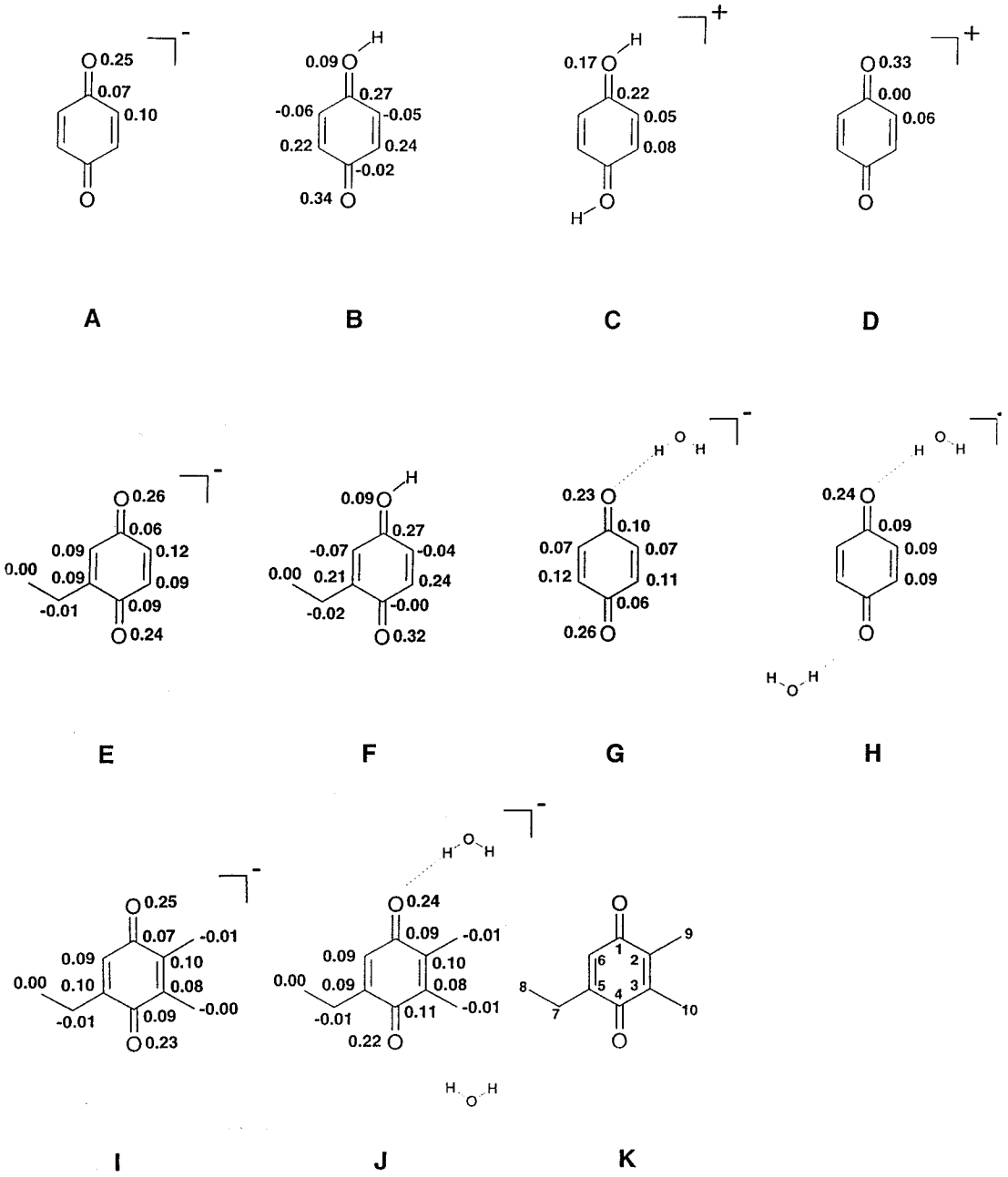

Figure 1. Schematic representations and computed total spin density distributions of the quinones investigated in the present work: (A) 1,4-benzoquinone radical anion (Q^-); (B) protonated Q^- (QH); (C) doubly protonated Q^- (QH_2); (D) 1,4-benzoquinone radical cation; (E) 5-ethyl-1,4-benzoquinone anion radical (QEt^-); (F) singly protonated QEt^- (QEtH); (G) Q^- hydrogen bonded to a single water; (H) Q^- hydrogen bonded to two water molecules; (I) plastoquinone radical anion (psQ^-); (J) psQ^- hydrogen bonded to two water molecules; (K) atomic labeling used throughout. Spin densities are from PWP86/6-311G(2d,p) calculations on B3LYP/6-311G(d,p) optimized geometries.

values) on all the hydrogens and hence not included in Table 1. For the quinone anion radical, the main part of the unpaired spin resides on the oxygens (0.252 on each), whereas the remainder is more or less evenly distributed on the carbon atoms ($\leq$0.1 on each carbon). The negative charge is localized to the two oxygens (-0.49), whereas the charges on C1 and C4 are $+0.30$ and -0.13 on each of the remaining four carbons. These data, from the PWP86/6-311G(2d,p) calculations, differ somewhat from the B3LYP/6-311+G(2df,p) results. The latter predict larger charges on the oxygens (-0.54) and also negative charges on the C1/C4 carbons, ca. -0.18, whereas the remaining carbons in this case carry a slight positive charge. The spin distributions are however highly similar between the two methods.

The presence of a singly hydrogen-bonding moiety distorts the spin distribution such that less spin is found at the H-bonding oxygen (O1) than at the oxygen not involved in the hydrogen bonding (O4). The carbon spin distribution attains more of an alternating character, with more spin on C1, C3, and C5 and less on C2, C4, and C6. Adding a second water molecule, at the O4 end, again makes the spin distribution symmetric. There is slightly less spin on the oxygens, compared with the free anion radical, and a more homogeneous distribution of spin on the carbon atoms.

Ethylation casuses a small distortion to the spin and charge distribution in the anion radical. The unpaired spin on O1/O4 is split from 0.252/0.252 to 0.255/0.239, and also the carbons display a slightly distorted spin distribution. Part of the negative charge is moved out to the ethyl tail, and the ring carbons attain a more asymmetric charge distribution. For the cation radical, the spin localization is even larger toward the oxygens (0.33

TABLE 4: Hyperfine Coupling Constants of the 1,4-Benzoquinone Anion, Cation, and Singly and Doubly Protonated Anions (G): PWP86/6-311G(2d,p)//B3LYP/6-311G(d,p) Calculations

atom	A_{iso}	T_{xx}	T_{yy}	T_{zz}	A_{iso}	T_{xx}	T_{yy}	T_{zz}
	Q^-				Q^+			
C1	−3.7	−3.1	−1.8	4.9	−9.4	−3.8	0.3	3.4
C2	−0.1	−2.8	−2.7	5.6	21.8	−2.9	−2.4	5.4
C3	−0.1	−2.8	−2.7	5.6	21.8	−2.9	−2.4	5.4
C4	−3.7	−3.1	−1.8	4.9	−9.4	−3.8	0.3	3.4
C5	−0.1	−2.8	−2.7	5.6	21.8	−2.9	−2.4	5.4
C6	−0.1	−2.8	−2.7	5.6	21.8	−2.9	−2.4	5.4
O1	−8.2	−27.7	13.8	14.0	−8.7	−33.2	15.6	17.6
O4	−8.2	−27.7	13.8	14.0	−8.7	−33.2	15.6	17.6
H2	−2.5	−1.3	−0.8	2.1	18.1	−1.7	0.3	1.4
H3	−2.5	−1.3	−0.8	2.1	18.1	−1.7	0.3	1.4
H5	−2.5	−1.3	−0.8	2.1	18.1	−1.7	0.3	1.4
H6	−2.5	−1.3	−0.8	2.1	18.1	−1.7	0.3	1.4
	QH				*t*-QH_2^+			
C1	8.6	−8.9	−8.6	17.6	2.8	−7.5	−7.1	14.7
C2	−6.6	−2.0	0.7	1.3	−2.2	−1.7	−1.4	3.2
C3	6.0	−6.7	−6.4	13.1	−0.7	−2.9	−2.6	5.4
C4	−9.6	−0.9	−0.2	1.1	2.8	−7.5	−7.1	14.7
C5	4.8	−6.0	−5.7	11.7	−2.2	−1.7	−1.4	3.2
C6	−6.4	−2.1	0.9	1.3	−0.7	−2.9	−2.6	5.4
O1	−4.6	−13.2	6.4	6.8	−7.0	−20.5	10.0	10.5
O4	−10.3	−36.6	18.3	18.3	−7.0	−20.5	10.0	10.5
H2	0.8	−1.0	0.0	1.0	−1.7	−1.1	−0.9	2.0
H3	−5.9	−3.0	−0.8	3.7	−2.6	−1.5	−1.0	2.5
H5	−5.3	−2.6	−0.8	3.4	−1.7	−1.1	−0.9	2.0
H6	0.8	−1.0	0.0	1.0	−2.6	−1.5	−1.0	2.5
H1	−2.4	−2.7	−1.6	4.3	−4.0	−4.4	−2.2	6.6
H4					−4.0	−4.4	−2.2	6.6

on each), whereas the carbons have very little spin. The positive charge is located on the C1/C4 carbons and the ring protons.

In the neutral ("protonated anion") radical QH, the radical character of the protonated oxygen (O1) is removed, and the system thus resembles more the odd-alternant radical of phenol in terms of its spin distribution. Starting from the C1 position, the ring carbons hold alternatingly > 0.2 and < −0.1 unpaired electrons, and the radical oxygen O4 holds ca. 0.34. Again, ethylation distorts the picture slightly.

In the doubly protonated radical QH_2^+, finally, the majority of the unpaired spin is localized to the C1/C4 carbons (ca. 0.22 on each) and in part to the oxygens. The doubly bonded carbons hold very little unpaired spin. The pairwise symmetric distribution (C2/C5 0.05; C3/C6 0.08) is caused by the local cis/trans influence of the OH protons. The PWP86 calculations predict that the positive charge resides almost entirely at the C1/C4 positions (and some at the hydroxy protons), as in the case of the ionized quinone, Q^+. At the B3LYP level, more of the positive charge is placed on the ring protons.

Hyperfine Structures. The key experimental techniques to analyze the presence and nature of the quinones in biological systems are based on electron spin resonance (ESR) and related magnetic resonance techniques. We have therefore computed the hyperfine coupling constants for a number of the different quinone radicals investigated in the present work (Tables 4−6). These are compared with available experimental data for model quinone systems (Table 7), observed in a variety of solvents. The theoretical data reported are from the PWP86/6-311G(2d,p)//B3LYP/6-311G(d,p) calculations. We also include data for the quinone anion radical hydrogen bonded to water.

There have been several studies of the hyperfine properties of free quinone anion radicals, their protonated counterparts, and various alkylated species.[6−13,44,45] Data are available for the protons as well as for ^{13}C and ^{17}O enriched quinones, and measurements have been made in a wide range of solvents and frozen alcohol solutions. The solvent studies show a strong

TABLE 5: Hyperfine Coupling Constants of the Singly and Doubly Hydrogen-Bonded 1,4-Benzoquinone Anion (G): PWP86/6-311G(2d,p)//B3LYP/6-311G(d,p) Calculations

		$Q^-(H_2O)$				$Q^-(H_2O)_2$		
atom	A_{iso}	T_{xx}	T_{yy}	T_{zz}	A_{iso}	T_{xx}	T_{yy}	T_{zz}
C1	−2.4	−4.1	−2.9	7.0	−2.6	−3.8	−2.5	6.3
C2	−0.9	−2.3	−2.1	4.3	−0.1	−2.7	−2.5	5.2
C3	0.8	−3.2	−3.1	−6.3	−0.1	−2.7	−2.5	5.2
C4	−4.7	−2.8	−1.5	4.3	−2.6	−3.8	−2.5	6.3
C5	0.8	−3.3	−3.2	6.5	−0.1	−2.7	−2.5	5.2
C6	−1.0	−2.4	−2.1	4.5	−0.1	−2.7	−2.5	5.2
O1	−8.6	−25.8	12.7	13.1	−8.3	−26.8	13.2	13.6
O4	−8.7	−28.9	14.4	14.5	−8.3	−26.8	13.2	13.6
H2	−2.0	−1.1	−0.8	1.9	−2.4	−1.3	−0.8	2.1
H3	−2.8	−1.5	−0.8	2.2	−2.4	−1.3	−0.8	2.1
H5	−2.9	−1.5	−0.8	2.3	−2.4	−1.3	−0.8	2.1
H6	−2.1	−1.1	−0.8	1.9	−2.4	−1.3	−0.8	2.1
H_{Hbond}	0.0	−1.1	−1.0	2.2	0.0	−1.1	−1.0	2.2
O_{Water}	0.4	0.0	0.0	0.0	0.3	−0.1	0.0	0.1
H'_{Water}	0.1	−0.4	−0.3	0.7	0.0	−0.5	−0.3	0.8

TABLE 6: Hyperfine Coupling Constants of the Ethylated 1,4-Benzoquinone Anion and Singly Protonated Counterpart (G): From PWP86/6-311G(2d,p)//B3LYP/6-311G(d,p) Calculations

	QEt^-				QEtH			
atom	A_{iso}	T_{xx}	T_{yy}	T_{zz}	A_{iso}	T_{xx}	T_{yy}	T_{zz}
C1	−4.2	−3.1	−1.8	4.9	8.0	−8.9	−8.5	17.5
C2	0.5	−3.3	−3.2	6.5	−6.4	−1.3	0.4	0.9
C3	−0.3	−2.9	−2.7	5.6	5.7	−6.8	−6.5	13.3
C4	−3.1	−3.6	−2.5	6.1	−8.5	−1.3	0.5	0.8
C5	−0.1	−2.6	−2.5	5.0	5.1	−5.7	−5.4	11.1
C6	−0.4	−2.5	−2.4	4.9	−6.6	−2.6	1.1	1.5
O1	−8.5	−27.9	13.8	14.1	−3.8	−12.9	6.3	6.6
O4	−7.6	−26.0	12.8	13.1	−9.5	−33.7	16.8	16.9
H2	−3.0	−1.6	−0.8	2.3	0.3	−1.0	−0.1	1.1
H3	−2.5	−1.4	−0.8	2.1	−6.1	−3.1	−0.8	3.9
H6	−2.2	−1.1	−0.8	1.9	0.9	−1.0	0.0	1.0
H1					−2.4	−2.6	−1.6	4.2
C7	−1.4	−0.2	−0.1	0.3	−2.4	−0.2	0.0	0.2
H7(2)	2.7	−0.7	−0.3	1.1	7.2	−0.9	−0.4	1.2
C8	−0.1	−0.1	0.0	0.1	−0.2	−0.1	−0.1	0.2
H8(3)	0.0	−0.3	−0.2	0.5	−0.1	−0.3	−0.2	0.6

TABLE 7: Experimentally Observed and Previously Calculated Hyperfine Coupling Constants of 1,4-Benzoquinone Radicals (G)

	experiment				
atom	Q^-	QMe^-	QH	QH_2^+	B3LYP/DZP′ Q^-
C1(2)	−2.1 to +0.2				−3.7
C2(4)	−0.1 to −0.7				−0.1
O1(2)	−8.6 to −9.5			−7.8	−7.2
H2	−2.7[a]	−2.7	0.3	−2.1	-2.3
H3	−2.7	−2.4	5.1	−2.5	−2.3
H5	−2.7		5.1	−2.1	−2.3
H6	−2.7	−2.0	0.3	−2.5	−2.3
H1				−3.3	
H_{Hbond}	0.1[b]				
H_β(av)		2.7			
ref	5−7,12,45	5,11	7	7	25

[a] Full hf tensor is −3.6, −1.4, −3.2 G. [b] Full hf tensor is 2.1, −1.0, −1.0 G.

dependence, in particular in ^{13}C and ^{17}O hyperfine structures, on the dielectricity of the medium.[6,11,13,45] Frozen alcohol solution ESR and ENDOR studies[8,9,12] have shown the presence of hydrogen bonding to the quinone oxygens (one per oxygen[9]), located at normal H-bonding distances and with C═O−H bond angles close to 180°.

For the four α-protons in Q^-, O'Malley and Babcock reported the hf tensor −10.2, −3.9, −9.0 MHz, with an isotropic component of −7.7 MHz (−2.7 G).[12] This agrees well with

the presently computed data of $A_{iso} = -7.0$ MHz and the full tensor −10.7, −1.1, −9.2 MHz. Adding a single hydrogen-bonding water molecule leads to large asymmetry in the carbon hyperfine structure owing to the shift to the odd-alternant type of spin distribution. The four α-protons become pairwise equivalent. The difference in resulting hyperfine components should be sufficiently large to be detected experimentally. No such asymmetry was however reported in the frozen solution studies by O'Malley and Babcock, indicating that the system does not carry a single hydrogen bond. Addition of a second water molecule leads again to a symmetric situation with hyperfine splittings almost identical to those of the free quinone anion radical (cf. Tables 4 and 5). The calculated full hyperfine tensor for both the hydrogen bonding protons are −3.1, −2.8, +6.2 MHz with a near-zero isotropic component and are the same for both the singly and doubly hydrogen-bonded systems. This can be compared with the ENDOR data of −2.8, −2.8, +5.9 MHz and $A_{iso} = +0.1$ MHz.[12]

Studies of solvent effects on the heavy atom hfcc's have shown that the isotropic ^{17}O component is reduced in magnitude as the dielectric constant of the medium increases (from −9.53 G in DMF to −8.58 G in water).[6] For the C1/C4 carbons the isotropic value changes from −2.1 G in DMSO to +0.2 G in water, whereas for the four C2 carbons the shift is −0.1 → −0.7 G.[13] The presence of the two hydrogen-bonding water molecules in the present calculations causes a shift in isotropic coupling on C1/C4 by 1.1 G toward more positive values. For the remaining ring carbons no shifts toward more negative isotropic couplings are observed from the hydrogen bonding. For the oxygens, the presence of two hydrogen bonds leads to numerically slightly larger values (−8.2 → −8.3 G), opposite the effect observed when increasing the dielectricity of the medium. Possibly, water atoms interacting directly with the ring π-system might underlie the experimentally observed shift; such water molecules have not been included in the present work.

The α-proton hfcc's undergo only minor modifications upon altering the dielectricity of the solvent. The hydrogen-bonding water molecules shift the α-proton isotropic couplings from −2.5 G (free anion) to −2.4 G (2 water molecules present), in nice agreement with the measured solvent effects (−2.42 G in DMSO, −2.36 G in H_2O).[13] The effects of increasing dielectric constants of the solvent have been calculated by Spanget-Larsen at the INDO level[26] and found to agree well with experiment. This indicates that the model with only two water molecules is sufficient in terms of the hydrogen-bonding effects but insufficient to model the total solvent effects. The vaccuum calculations in the present work seem to agree slightly better with the water solvent data for the oxygens, but with the less polar solvents for the carbon atoms. The isotropic couplings of Q^- are at the B3LYP/6-311+G(2df,p) level −2.2 (H), −6.4 (O), −3.3 (C1) and −0.4 (C2) G, respectively, and −2.1 (H), −6.4 (O), −2.5 (C1) and −0.5 (C2) G in the presence of the two hydrogen-bonding water molecules. The shifts in isotropic hfcc caused by the hydrogen bonding moieties are hence very similar between the B3LYP and the PWP86 calculations.

Ethylation of Q^- causes a split of the four equivalent α-protons. Measurements have been made of, for example, the proton couplings in methyl-substituted quinone anion radicals (QMe^-),[5] which showed that the α-proton hfcc's split from four equivalent couplings of −2.7 G[12] to three protons with isotropic couplings −2.70, −2.44, −1.95 G. This is nicely reproduced in the present work (−3.0, −2.5, −2.2 G).

Protonation of the quinone anion modifies the hyperfine structure considerably. Due to the odd-alternant character of the spin distribution in QH, all carbons attain large isotropic couplings (±4−10 G) and also a considerably increased anisotropy. The α-proton couplings split up into two large components (−5 G, at the C4 end) and two near-zero couplings at the protonated end. The experimental isotropic couplings for the α-protons are 5.1 and 0.3 G, respectively,[7] in good agreement with the computed data. The calculated hyperfine coupling on the added hydroxy proton is ca. −2.4 G and displays relatively large anisotropy. There is furthermore a large separation of the two oxygen hfcc's (isotropic values: O1, −4.6; and O4, −10.4 G). The overall hf pattern thus resembles that of the phenoxyl radical,[29] although the couplings are smaller for all atoms but the radical oxygen (O4). Ethylation of QH again causes minor adjustments to the hyperfine couplings. In particular, the β-protons attain large isotropic components (7.2 G).

For the doubly protonated system the isotropic components to the carbon atoms decrease significantly to within ±3 G. The oxygen couplings are numerically smaller than for the anion radical (−7.0 vs −8.3 G), although still considerable. The reduction in oxygen couplings upon protonation has also been observed experimentally: from −8.6 to −9.5 G in Q^- to −7.8 G in QH_2^+.[13] For the α-protons the isotropic components decrease by ca. 0.12 G compared with the anion radical[7] and split pairwise into the hf pattern 2 × −2.4 and 2 × −2.1 G for the cis form and 2 × −2.5 and 2 × −2.1 G for the trans conformer.[46] The calculated values are 2 × −2.4 and 2 × −1.8 vs 2 × −2.6 and 2 × −1.7 G, respectively. The calculations hence tend to overestimate the effects of protonation to the induced hyperfine couplings on the α-protons. On the other hand, the computed average value for the four α-protons (−2.15 G) matches perfectly the averaged data reported for QH_2^+ in trifluoroacetic acid at $T = 20$ °C, 2.16 G.[47] A_{iso} for the two hydroxy protons have been reported as 3.2−3.4 G in various acidic solvents at room temperature (cf. ref 47 and references therein). The calculated values are slightly too large, −4.0 G, which in part may be explained in terms of solvent interactions and vibrational averaging at the relatively high temperatures.

Plastoquinone Models. Detailed understanding of the energetics and reactions of plastoquinones is of vital importance for the understanding of photosynthesis, as they form the key linkages between PSII and PSI. One of the main aspects here is the presence or absence of hydrogen bonding. This will largely modify both electronic properties, such as electron affinity and reduction potential, and the mobility of the quinone. The plastoquinone model used in the present work is similar to those used previously by Wheeler et al.[19] and by O'Malley and Collins.[25] The difference is the length of the alkyl tail at the 5 position. In the present work we truncate the tail at the second carbon atom; Wheeler and co-workers used a propene group in order to model the effects of the double bond between the second and third carbon, whereas O'Malley and Collins extended the model further by substituting the two terminal propene hydrogens by methyl groups. Since no hyperfine couplings have been detected beyond the γ position (C8 in our model), we believe that the present truncated model is reasonable.

Zheng and Dismukes[16] have shown that the relative orientation differs between quinones in PSII (tail in plane) and in bacterial reaction centers (tail perpendicular to quinone ring plane). Based on this, we initially assumed in our calculations that the ethyl tail was located in the ring plane, although not explicitly constraining it to this position in the optimizations. In both of the previous theoretical models,[19,25] an out-of-plane arrangement was assumed, leading to erronous hyperfine patterns for the β-protons.

TABLE 8: PWP86/6-311G(2d,p)//B3LYP/6-311G(d,p) Calculated Hyperfine Coupling Constants (G) for the Plastoquinone Model Anion, without and with Hydrogen Bonding. Experimental Data for Model Plastoquinones and Q_A^- in PSII.[14−16] Previously Calculated Isotropic Data for Model Plastoquinone Anion at B3LYP/[632/41] level[19]

	psQ$^-$			psQ$^-$(H$_2$O)$_2$			PQ-9$^-$ (exp)			Q_A^- (exp)			ref 19
atom	A_{iso}	T_{xx}	T_{zz}	A_{iso}	T_{xx}	T_{zz}	A_{iso}	T_{xx}	T_{zz}	A_{iso}	T_{xx}	T_{zz}	A_{iso}
C1	−3.5	−3.4	5.6	−2.8	−3.9	6.8							−3.5
C2	0.5	−2.9	5.7	0.0	−2.9	5.6							0.7
C3	−0.1	−2.5	4.8	−0.8	2.4	4.6							−0.8
C4	−2.2	−3.9	6.7	−0.2	−2.6	5.1							−2.1
C5	0.3	−2.9	5.7	−0.6	−2.5	4.8							0.1
C6	−0.5	−2.7	5.2	−1.1	−4.4	8.0							−0.1
O1	−8.3	−27.1	13.7	−8.7	−26.0	13.2							−7.5
O4	−7.5	−25.2	12.8	−8.4	−24.3	12.3							−7.2
H6	−2.4	−1.2	2.0	−2.2	−1.2	2.0	−2.1	−1.2	2.0	−2.0	−0.7	2.4	−2.3
C7	−1.7	−0.2	0.3	−1.6	−0.2	0.3							−1.3
H7 (2)	3.0	−0.8	1.1	2.8	−0.8	1.1	2.5	−0.1	0.2	2.4/2.6	−1.5	2.8	1.1
C8	−0.1	−0.1	0.1	−0.2	−0.1	0.1							0.8
H9	−0.1	−0.2	0.4	−0.1	−0.2	0.4	−0.1						−0.1
H(C9) (3)	2.2	−0.6	0.9	2.2	−0.6	0.9	2.3	−0.4	0.8	2.1	−0.4	0.7	2.1
H(C10) (3)	1.9	−0.6	0.9	1.8	0.6	0.9	1.7	−0.4	0.7	1.6	−0.4	0.8	1.5
$H_{Hbond}1$				0.1	−1.2	2.2	0.0	−0.9	1.8	0.0	−0.8	1.6	
$H_{Hbond}2$				0.1	−1.2	2.3	0.5	−0.8	1.6	0.3	−0.7	1.4	

The additional methyl groups at the C2 and C3 positions result in further geometric distortions to the ring, relative to QEt$^-$, such that the bonds near the methylated site increase by ca. 0.01 Å and the bonds adjacent to the ethylated site decrease. The bond angles in the ring adjust accordingly. Compared with the previous plastoquinone anion models studied, the geometries are very similar. The larger basis set used in the present optimization calculations leads, however, to slightly shorter bonds. Hydrogen bonding to the oxygens lengthens the C═O bonds slightly (to 1.271 and 1.272 Å, respectively) and also introduces a larger difference between the two C═C double bonds than for free psQ$^-$. The oxygen atoms bend away somewhat from the water/methyl sides. The hydrogen-bonding water molecules are oriented such that one lies slightly above and the second slightly below the quinone ring plane (O−H−O angle 167°). The H-bonding distances are 1.78 Å and the C═O−H bond angles 141−143°. The geometries of the water molecules and their relative positions are very nearly identical. We also note that the water molecules in psQ$^-$ fall in a cis position relative to each other, whereas their optimized positions in the interaction complex with Q$^-$ are trans. This difference is possibly caused by the presence of the ethyl tail in psQ.

The presence of the two hydrogen-bonding moieties perturbs the spin distribution in psQ$^-$ very little, in the order of 0.01−0.02. On the other hand, the effects on the electron affinity of psQ are significant. The electron affinity of free psQ is ca. 0.3 eV less than for the free, unsubstituted 1,4-benzoquinone. For Q, the two hydrogen-bonding water molecules were however shown to raise the EA by 0.6 eV. In psQ, the difference is even larger than in the unsubstituted benzoquinone by ca. 1 kcal/mol.

Recent EPR and ENDOR studies predict the remaining α-proton H6 to have an isotropic component of −2.05 G.[14−16] The calculated values are −2.2 G for H6 in QEt$^-$ (Table 6), −2.4 G in psQ$^-$, and −2.2 G in psQ$^-$(H$_2$O)$_2$ (Table 8). The anisotropic data for both systems are in excellent accord with the experimental results for the plastoquinone model PQ-9$^-$ in frozen propanol.[14,15] In PSII, the isotropic component for Q_A^- is slightly smaller, and the anisotropic tensor displays less axial symmetry than the model plastoquinones.[16]

The two β-protons in our models, labeled H7 in Table 8, are oriented symmetrically with one proton above and one below the plane of the quinone ring. The computed hyperfine tensor components are highly similar between the QEt$^-$, psQ$^-$, and psQ$^-$(H$_2$O)$_2$ systems. The presence of the two methyl groups leads to an increase in the isotropic component (psQ$^-$ vs QEt$^-$), whereas the two hydrogen-bonding groups induce small reduction in $A_{iso}(H_\beta)$. In liquid solution, there will most likely be some degree of vibrational motion about the C5−Cβ bond, which may cancel out the anisotropic contributions to the hf splittings. No anisotropic data were reported in the ENDOR studies of PQ-9$^-$.[15] Rigby et al.[14] report only on one component in their ENDOR and TRIPLE measurements on Q_A^-, as $A_\perp$ = 2.9 G. This could be the A_{yy} component of psQ$^-$ (2.7 G; 2.5 G in psQ$^-$(H$_2$O)$_2$), although more data are needed in order to determine this more exactly. Zheng and Dismukes reported full tensors for the PQ-9$^-$ β-protons in 2-propanol and could show that the anisotropic components were very small ($|T_{ii}|$ = 0.1−0.2 G).[16] Since the computed values are larger by a factor 10, a vibrational averaging may be a plausible explanasion for the observed small anisotropies.

In PSII Q_A^-, Zheng and Dismukes used computer simulations of the ESR spectra to determine the tensors 3.3, 3.3, 15 and 2.7, 2.7, 15 MHz for the two β-protons respectively.[16] These were based on two experimentally observed couplings of 3.3 and 2.7 MHz, tentatively assigned to the $A_\perp$ components of the two β-hydrogens and the isotropic value (ca. 7 MHz) observed for Hβ in PQ-9$^-$. The calculated anisotropic components deviate a bit too much from the experimental data, especially in the T_{zz} component. The calculations furthermore predict the anisotropic tensor to be nearly rhombic (−0.8, −0.2, 1.0 G for psQ$^-$) rather than the nearly axially symmetric model (−1.5, −1.3, 2.8 G) suggested by Zheng and Dismukes.

MacMillan et al., finally, reported in their EPR and ENDOR study of Q_A^- in PSII, two peaks at 5.8 and 9.2 MHz, which could be assigned to the $A_\perp$ and $A_{||}$ components of a methylene proton.[15] This agrees rather well with the computed data for psQ$^-$(H$_2$O)$_2$, (5.8, 6.9, 10.9 MHz), although, again, the amount of experimental data is not sufficient provide a definite and final conclusion.

The two methyl groups in both the PQ-9 model and in Q_A are expected to rotate freely. In both systems these have been shown to differ slightly, such that the rotationally averaged isotropic component of one is ca. 1.5 MHz larger than the other. Based on arguments of resonance structures and influence of two inequivalent hydrogen bonds (see below), the larger component has been assigned to the methyl group in the 3 position and the smaller at the 2 position. Both previous[19,25] and the present theoretical results show, however, that the ordering is the opposite. The present data also clearly reveal

that the effects of hydrogen bonding on the hyperfine couplings of the methyl group hydrogens are minute. Instead, the difference between the two methyl groups is caused by the presence of the alkyl tail at the C5 position. The computed data for both psQ^- and $psQ^-(H_2O)_2$ agree very well with the experimental PQ-9^- and Q_A^- hfcc's.

The second important aspect of the quinones, besides the relative orientation of the ring and the alkyl tail, is the presence and location of hydrogen-bonding groups. In the present work, both water molecules attain similar couplings, due to their similar geometries and orientations relative to the quinone (Table 8). The agreement with the reported data is fair for one of the protons. The second hydrogen-bonding moiety is thought to be located above or below the ring plane rather than in the plane of the quinone ring, thereby resulting in a slightly larger isotropic coupling.[15] The deviations from the present, symmetric model supports such an argument. What the calculations have shown is, however, that hydrogen-bonding groups are not hindered by the bulky substituent groups on the quinone, as has been argued; rather, the effect appears to be caused by, for example, the location of hydrogen-bonding side groups, which may be restricted and unable to attain the optimum position for hydrogen bonding. As mentioned above, hydrogen-bonding effects are most important primarily as they increase the electron affinity of the system by some 15 kcal/mol. We stress, though, that all of the present calculations are performed *in* vacuo and that the inclusion of a solvent model may modify this value.

Energetic Considerations. Both the electron affinities and the bond strengths to hydrogen atoms for quinones are of importance for the function of PSII. The primary reaction sequence following photon absorption leads to the formation of the P_{680}^+ cation and the Q_A^- anion. The ease and the energy required for this process depend critically on the electron affinity of Q_A. The present calculations, in which we use large basis sets and include zero-point vibrational effects, gave electron affinities of 41 and 47 kcal/mol for psQ and Q, respectively. These are surprisingly large values of the electron affinity for stable closed shell molecules and is clearly the reason that a quinone is used as an acceptor in this position in PSII. The experimental value for the electron affinity of 1,4-benzoquinone is 44 ± 2 kcal/mol.[42] A principal conclusion from the above analysis of the hfcc in comparison to the experimental measurements on PSII is that Q_A is hydrogen bonded at both oxygens. This effect is also quite significant in the electron-transfer process from P_{680}, since this increases the electron affinity of Q_A. The increase obtained from the calculations is 15 kcal/mol to a final electron affinity of 58 (psQ) or 62 (Q) kcal/mol. To this value should be added long-range dielectric effects which will further increase the electron affinity. These considerations will be discussed in more detail in another paper on the overall energetics of the reactions in PSII.[48] Following its reduction, Q_A^- subsequently transfers an electron to Q_B to produce Q_B^-. From the present results, the driving force for this electron transfer is unlikely to be a substantially more favorable hydrogen-bonding arrangement for Q_B, since hydrogen bonding at Q_A already plays a critical energetic role. This agrees well with the findings for photosynthetic bacteria, where Lubitz et al. have shown that Q_A appears to be more strongly H-bonded than is Q_B.[49]

The second step in the reaction sequence involves uptake of a proton from the stroma by Q_B^- and the transfer of a second electron via Q_A to form $Q_A(Q_BH)^-$. Subsequent protonation forms the neutral Q_BH_2 molecule, which dissociates from its binding site to transport both protons and electrons across the thylakoid membrane. In this capacity, its movement contributes directly to the chemiosmotic gradient used in ATP production. QH_2 is an efficient proton carrier, since it lacks both charge and essentially also dipole moment. It is therefore not likely to form any strong bonds to any molecule on the way. The mechanism for the proton-coupled electron transfer to Q_B^- has been investigated in detail in reaction centers of *Rb. sphaeroides*.[50] Based on quinone substitution studies in the Q_A site, it was concluded that the process proceeds as either proton transfer followed by a rate-limiting electron transfer from Q_A^- to neutral Q_BH or as a concerted proton+electron transfer. From their experiments, the formation of a doubly charged intermediate Q_B^{2-} was definitely ruled out. The findings by Paddock et al. are confirmed in the present work, in that the second electron affinity ($Q^- \rightarrow Q^{2-}$) is energetically very costly. The calculations give at hand that the EA of Q^- is in fact negative (Table 3); this value should approach zero in the infinite basis set limit. From the calculations we can however conclude that Q^{2-} is unlikely to be formed, although stabilizing dielectric effects are significant also in a relatively nonpolar environment as the interior of a protein. Whether the process is two-step $H^+ + e^-$ or a concerted reaction cannot be determined from the calculations. The computed data indicate that the proton affinity of Q^- is very high and that the EA of QH is only ca. 7 kcal/mol less than for Q. The Q_BH^- complex, once formed, will easily extract its second proton to form QH_2.

QH_2 eventually loses both hydrogen atoms, either through H-transfer or as protons+electrons (see below). In this context, the bond strength between Q and the two hydrogen atoms is quite significant. The present results gives a first hydrogen atom bond strength ($QH_2 \rightarrow QH + H$) of 84.5 kcal/mol and a second bond strength ($QH \rightarrow Q + H$) of 64.2 kcal/mol. The second hydrogen atom bond strength is probably weak enough so that the hydrogen atom could be accepted by the ferredoxin, FeS, center of the cytochrome b_6f complex either directly by protonation of a bridging sulfur during reduction of the cluster or by protonation of an acid/base group in the immediate vicinity of the cluster. Recent calculations on Fe_4S_4 clusters with different oxidation states indicate that the bridging sulphurs can bind hydrogen atoms by over 60 kcal/mol.[51] However, the first hydrogen bond strength in QH_2 of 84.5 kcal/mol is too strong for ferredoxin to act as a coupled H^+/e^- acceptor.

Assuming instead that the process proceeds via reduction of the ferredoxin and the cytochrome, coupled with release of two protons to solution, the energetics in terms of ionization potentials of QH_2 and QH should be compared with the electron affinities of FeS and of the cytochromes. Such studies are currently under way. We note from the present calculations that the ionization potential of QH_2 is only 7.7 eV, i.e. that QH_2 is relatively easily ionized. This could speak in favor of the generally accepted electron+proton sequence for oxidation of QH_2 at the cytochrome b_6f complex. From the present calculations, we are not able to determine which of the two mechanisms is the more likely to occur. The data currently at hand imply that either mechanism (H-atom transfer or electron transfer coupled with proton donation to solution) is actually more or less equally probable, although we are aware that the H-transfer model is indeed rather controversial. Further studies, both theoretical and experimental, are needed to elucidate these particular aspects of the photosynthetic reaction sequence in green plants.

Conclusions

We have in the present work undertaken a detailed analysis of geometries, spin properties, and hyperfine structures of a large set of 1,4-benzoquinone and related radicals. The B3LYP/6-

311G(d,p) optimized geometric structures agree well with previous theoretical data (where available), and the ionization potentials and electron affinities of Q are in good agreement with experimental data. The effects of alkylation are generally rather small, although the symmetry with respect to geometry, spin distribution, and hyperfine properties of the unsubstituted quinone is lost.

Larger effects are seen from protonation, whereby the geometry around the protonated oxygen becomes significantly altered. The QH and QEtH radicals are odd-alternant radicals, with very strongly modified spin distributions and hyperfine structures compared with the unprotonated anion radical. Addition of a second proton gives spin and hyperfine patterns that are closer to those of the radical anion, yet sufficiently altered to allow for a clear distinction between the two. The computed hyperfine properties for Q^-, QH, QH_2^+, and the ethylated species agree very well with experimental data.

The effects of hydrogen bonding have been examined for the benzoquinone anion radical and a model plastoquinone anion radical. It is concluded that the two hydrogen-bonding groups (water molecules) in our models attain highly symmetric positions in their relative orientations to the quinone rings and that the HO fragment of the water molecules that are involved in the bonding lie in, or nearly in, the quinone ring plane. The plastoquinone models are compared with experimental data for the PQ-9^- model system in liquid and frozen solution and with data for Q_A^- in PSII. Overall, the computed hyperfine data compare best with that for the PQ-9 anion radical in frozen solution. The deviations compared with Q_A^- can to some extent be attributed to difficulties in obtaining well-resolved experimental spectra. The calculations show that the differences in hyperfine properties of the two methyl groups in psQ^- are related to the perturbations caused by the alkyl tail, and not by the presence of asymmetric hydrogen bonding. Calculations finally confirmed that one of the hydrogen-bonding groups observed in experiments is located in the plane of the quinone ring, whereas the other most likely is not.

The presence of the hydrogen-bonding groups increases the electron affinity of quinone/plastoquinone by ca. 15 kcal/mol. To correctly account for the energetics involving the steps of the electron transfer from the excited P_{680} unit in PSII, via Q_A and Q_B, to the quinone pool of the membrane, proton capture and QH or QH_2 transport through the membrane, and finally removal of hydrogen atoms and/or electrons+protons to the ferredoxine and cytocrome centers of PSII, hydrogen bonding to Q_A may be an essential ingredient.

Acknowledgment. The Swedish Natural Sciences Research Council (NFR), NIH (GM37300), the USDA CREO, and the Human Research Frontiers Program are gratefully acknowledged for financial support. We also acknowledge grants of computer time at the National Supercomputer Center (NSC) in Linköping, and the Center for Parallel Computing (PDC) at the Royal Institute of Technology, Stockholm.

References and Notes

(1) Diner, B. A.; Babcock, G. T. In *Oxygenic Photosynthesis: The Light Reactions*; Ort, D. R., Yocum, C. F., Eds.; Kluwer: Dordrecht, 1996; pp 213−247.
(2) Michel, H.; Deisenhofer, J. *Biochemistry* **1988**, *27*, 1.
(3) Allen, J. P.; Feher, G.; Yeates, T. O.; Komiya, H.; Rees, D. *Proc. Natl. Acad. Sci. U.S.A.* **1988**, *85*, 8487.
(4) Ermler, U.; Fritzsch, G.; Buchanan, S. K.; Michel, H. *Structure* **1994**, *2*, 925.
(5) Ayscough, P. B. *Electron Spin Resonance in Chemistry*; Methuen & Co Ltd: London, 1974.
(6) Broze, M.; Luz, Z.; Silver, B. L. *J. Chem. Phys.* **1967**, *46*, 4891.
(7) Dixon, W. T.; Murphy, D. *J. Chem. Soc., Faraday Trans.* **1972**, *72*, 1221.
(8) Hales, B. J. *J. Am. Chem. Soc.* **1975**, *97*, 5993.
(9) Hales, B. J. *J. Am. Chem. Soc.* **1976**, *98*, 7350.
(10) Neta, P.; Fessenden, W. *J. Phys. Chem.* **1974**, *78*, 523.
(11) Niethammer, D.; Kirste, B.; Kurreck, H. *J. Chem. Soc., Faraday Trans.* **1990**, *86*, 3191.
(12) O'Malley, P. J.; Babcock, G. T. *J. Am. Chem. Soc.* **1986**, *108*, 3995.
(13) Sullivan, P. D.; Bolton, J. R.; Geiger, W. E., Jr. *J. Am. Chem. Soc.* **1970**, *92*, 4176.
(14) Rigby, S. E. J.; Heathcote, P.; Evans, M. C. W.; Nugent, J. H. A. *Biochemistry* **1995**, *34*, 12075.
(15) MacMillan, F.; Lendzian, F.; Regner, G.; Lubitz, W. *Biochemistry* **1995**, *34*, 8144.
(16) Zheng, M.; Dismukes, G. C. *Biochemistry* **1996**, *35*, 8955.
(17) Chipman, D.M.; Prebenda, M.F. *J. Phys. Chem.* **1986**, *90*, 5557.
(18) Raymond, K. S.; Wheeler, R. A. *J. Chem. Soc., Faraday Trans* **1993**, *89*, 665.
(19) Wise, K. E.; Grafton, A. K.; Wheeler, R. A. *J. Phys. Chem.* **1997**, *101*, 1160.
(20) Boesch, S. E.; Wheeler, R. A. *J. Phys. Chem.* **1995**, *99*, 8125.
(21) Datta, S. N.; Mallik, B. *Int. J. Quantum Chem.* **1997**, *61*, 865.
(22) Boesch, S. E.; Grafton, A. K.; Wheeler, R. A. *J. Phys. Chem.* **1996**, *100*, 10083.
(23) Wheeler, R. A. *J. Am. Chem. Soc.* **1994**, *116*, 11048.
(24) Pople, J. A.; Beveridge, D. L.; Dobosh, P. A. *J. Am. Chem. Soc.* **1968**, *90*, 4201.
(25) O'Malley, P. J.; Collins, S. J. *Chem. Phys. Lett.* **1996**, *259*, 296.
(26) Spanget-Larsen, J. *Theor. Chim. Acta* **1978**, *47*, 315.
(27) Blomberg, M. R. A.; Siegbahn, P. E. M.; Styring, S.; Babcock, G. T.; Å kermark, B.; Korall, P. *J. Am. Chem. Soc.*, submitted for publication.
(28) Siegbahn, P. E. M.; Crabtree, R. H. *J. Am. Chem. Soc.* **1997**, *119*, 3103.
(29) Himo, F.; Gräslund, A.; Eriksson, L.A. *Biophys. J.* **1997**, *72*, 1556.
(30) Himo, F.; Eriksson, L. A. *J. Phys. Chem. B*, in press.
(31) Slater, J. C. *Quantum Theory of Molecules and Solids*; McGraw-Hill: New York, 1974.
(32) Becke, A. D. *Phys. Rev.* **1988**, *A38*, 3098.
(33) Vosko, S. H.; Wilk, L.; Nusair, M. *Can. J. Phys.* **1980**, *58*, 1200.
(34) Lee, C.; Yang, W.; Parr, R. G. *Phys. Rev.* **1988**, *B37*, 587.
(35) Becke, A. D. *J. Chem. Phys.* **1993**, *98*, 1372.
(36) Perdew, J. P.; Wang, Y. *Phys. Rev.* **1986**, *B33*, 8800.
(37) Perdew, J. P. *Phys. Rev.* **1986**, *B33*, 8822; **1986**, *B34*, 7406.
(38) Frisch, M. J.; Trucks, G. W.; Schlegel, H. B.; Gill, P. M. W.; Johnson, B. G.; Robb, M. A.; Cheeseman, J. R.; Keith, T. A.; Peterson, G. A.; Montgomery, J.A.; Raghavachari, K.; Al-Laham, M. A.; Zakrevwski, V. G.; Ortiz, J. V.; Foresman, J. B.; Cioslowski, J.; Stefanov, B. B.; Nanayakkara, A.; Challacombe, M.; Peng, C. Y.; Ayala, P. Y.; Chen, W.; Wong, M. W.; Andres, J. L.; Replogle, E. S.; Gomperts, R.; Martin, R. L.; Fox, D. J.; Binkley, J. S.; DeFrees, D. J.; Baker, J.; Stewart, J. P.; Head-Gordon, M.; Gonzalez, C.; Pople, J. A. *Gaussian 94*; Gaussian Inc.: Pittsburgh, PA, 1995.
(39) St-Amant, A.; Salahub, D. R. *Chem. Phys. Lett.* **1990**, *169*, 387. St-Amant, A.; Ph.D. Thesis, Université de Montréal, 1991. Salahub, D. R.; Fournier, R.; Mlynarski, P.; Papai, I.; St-Amant, A.; Ushio, J. In *Density Functional Methods in Chemistry*; Labanowski, J., Andzelm, J., Eds.; Springer: New York, 1991. Daul, C.; Goursot, A.; Salahub, D. R. In *Grid Methods in Atomic and Molecular Quantum Calculations*; Cerjan, C., Ed.; Nato ASI C142, 1993.
(40) Eriksson, L. A. *Mol. Phys.* **1997**, *91*, 827.
(41) *Handbook of Chemistry and Physics*, 77th ed.; Lide, D. R., Ed.; CRC Press: New York, 1996.
(42) Chowdhury, S.; Heinis, T.; Grimsrud, E. P.; Kebarle, P. *J. Phys. Chem.* **1986**, *90*, 2747.
(43) Lias, S. G., et al. *J. Phys. Chem. Ref. Data* **1988**, *17, suppl. 1*.
(44) Vincow, G.; Fraenkel, G. K. *J. Chem. Phys.* **1961**, *34*, 1333.
(45) Das, M. R.; Fraenkel, G. K. *J. Chem. Phys.* **1965**, *42*, 1350.
(46) Barabas, A. B.; Forbes, W. F.; Sullivan, P. D. *Can. J. Chem.* **1967**, *45*, 267.
(47) Eberson, L.; Hartshorn, M. P. *J. Chem. Soc., Perkins Trans. 2* **1995**, 151.
(48) Blomberg, M. R. B.; Babcock, G. T.; Siegbahn, P. E. M. To be published.
(49) Feher, G.; Isaacson, R. A.; Okamura, M. Y.; Lubitz, W. In *Antennas and Reaction Centers of Photosynthetic Bacteria*; Michel-Beyerle, M.-E., Ed.; Springer-Verlag: Berlin, 1985; pp 174-189.
(50) Graige, M. S.; Paddock, M. L.; Bruce, J. M.; Feher, G.; Okamura, M. Y. *J. Am. Chem. Soc.* **1996**, *118*, 9005.
(51) Siegbahn, P.E.M. To be published.